Unscented Transformation-Based Filters: Performance Comparison Analysis for the State Estimation in Polymerization Processes with Delayed Measurements

Rubén Galdeano, Mariano Asteasuain,* Mabel Sánchez

State estimation with delayed measurements is essential to the operation of polymer processes due to the limited availability of reliable online sensors and the unavoidable hold-up time in the acquisition of critical variables data. In this work, a two-timescale approach is applied to three filters based on the Unscented Transformation, the Unscented Kalman Filter, the Unscented Recursive Nonlinear Dynamic Data Reconciliation and the Reformulated Constrained Unscented Kalman Filter, in order to incorporate delayed measurements into their estimation scheme. A comprehensive comparative analysis is performed, which shows that the three of them have very good accuracy and convergence properties. However, the Unscented Kalman Filter performs better in terms of computational time.

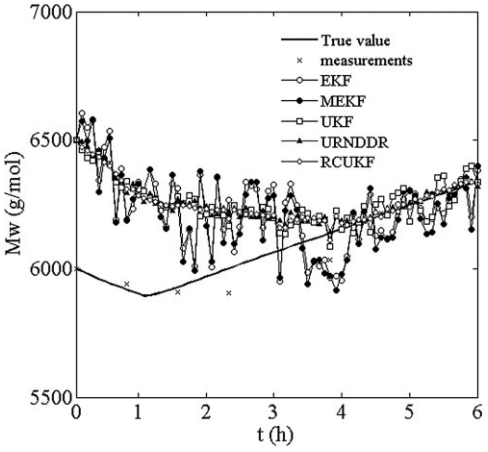

Introduction

One of the most important industries worldwide is the manufacturing of polymers, which is affected by an increasing demand for efficiency and competitiveness. This requires producing at the lowest cost possible while accomplishing stringent product specifications. In order to meet changing market demands, it must also be able to operate in a wide range of operating conditions without diminishing the quality of the products.

Dynamic operation is very significant in polymer manufacturing. On the one hand, a large number of polymers of industrial interest are produced by batch processes. On the other hand, continuous plants usually produce dozens of different materials using the same equipment. During the transition period between the steady-state production of one grade and another, off-spec material with little or no commercial value is generated. Therefore, the profitable operation of a polymerization plant demands to carry out such transitions as efficiently as possible.

However, dynamic operation of polymerization reactors is an extremely complex task. Polymerization processes usually exhibit highly exothermic reactions and changes in viscosity, causing complex heat-transfer dynamics and flow patterns. Moreover, these processes are strongly nonlinear. This has been reflected in the abundant production of design, optimization, and control of polymerization reactors studies found in the literature.[1,2]

One of the main difficulties in controlling the quality of polymers is the absence of reliable online sensors for some of their properties. Moreover, many important variables cannot be measured online or can only be measured at low sampling frequencies. Therefore, it is common that dynamic operation is performed following a set of trajectories obtained offline. However, uncertainty in

R. Galdeano, M. Asteasuain, M. Sánchez
Camino La Carrindanga km 7, Bahía Blanca, 8000, Argentina
E-mail: masteasuain@plapiqui.edu.ar

DOI: 10.1002/mren.201000060

process parameters and changing operating conditions, such as increased fouling of the reactor walls, changes in external and coolant temperatures, deactivation of catalysts, disturbances, etc., require these paths to be updated. This is especially important because the molecular properties of polymers, such as the molecular weight distribution (MWD), copolymer composition, etc., are very sensitive to operational conditions, and this affects the processing and end-use properties of the product.

The state estimation in a dynamic system is a technique that allows assessing inaccessible states through measurable variables. These variables can either be other states or any direct or indirect measured magnitude that make the system observable. Different techniques for nonlinear state estimation have been used for years in polymerization processes, such as the state estimation via nonlinear observers, data reconciliation, moving horizon estimation (MHE), neural networks, and fuzzy logic.[2–4] Comprehensive reviews of these can be found in Fonseca et al.[5] or in Richards and Congalidis.[1]

As the last mentioned review work indicates, an approach investigated by several researchers is the use of Kalman filtering. For continuous polymerization processes, for example, Schuler and Suzhen[6] estimated states using Extended Kalman Filtering (EKF) in a styrene polymerization process through easily measured process variables. Choi and Khan[7] also used this filtering technique in a continuous polymerization process for poly(ethylene terephthalate) (PET) manufacturing, comparing the estimates using only two online measurements with those obtained with the addition of five delayed offline measurements. They showed that the last option significantly improved the estimation. Sirohi and Choi[8] applied two different strategies online, the EKF and the estimation using nonlinear programming (NLP) techniques, to evaluate not only the states but also key system parameters in a continuous polymerization process. Also Mutha et al.[9] applied a multirate state estimator on a methyl methacrylate (MMA) solution polymerization. They used an EKF with fixed-lag smoothing that presents better convergence in comparison with the standard EKF due to its ability to reuse a measurement multiple times. The procedure is well suited for systems with delayed measurements. Recently, Li et al.[10] proposed a hierarchical Kalman filter to estimate state variables and kinetic parameters in a continuous ethylene/propylene/diene monomer (EPDM) rubber polymerization reactor.

Despite being a very used technique, the EKF may present numerical implementation problems when applied to complex systems.[11] The EKF approximates the actual probability distributions of the states by a Gaussian distribution. The first moment of the distribution is propagated through the nonlinear model, while the second one is spread through a linearized version of it. When this model is highly nonlinear, this approach may generate expectations and covariances of states wide departed from their actual values, which in the worst case can cause the divergence of the filter. Another disadvantage of the EKF is the need for computing the linearized Jacobian matrix of the states, which results in high computational costs. Several variants of the standard EKF are reported in the literature that aim at reducing its drawbacks. They are based, for instance, on the use of solution refinement, series Taylor expansion to the second order, geometrically adapted correction terms based on an invariant output error, reduction of the system model order, etc.[11]

In addition, in recent years two major branches emerged that aimed at solving EKF filtering problems. The first of them, supported by a theory dated back to several years but that has resurfaced, is the family of particle filters. Rawlings and Bakshi[12] made a review and applied these techniques to different processes. Chen et al.[13] also used this method in a batch reactor of MMA. The biggest drawback of the particle filters is the high computational time, which increases exponentially with the number of states to be estimated.

The second technique that has shown promising results is the family of filters based on a statistical concept known as the Unscented Transformation (UT) whose most known variant is the Unscented Kalman Filter (UKF). The UT is founded on the intuition that it is easier to approximate a probability distribution than it is to approximate an arbitrary nonlinear function or transformation. The approach takes a set of deterministically points and estimates their mean and covariance.[14] While EKF propagates the mean and covariance only with a first order accuracy, the UKF is accurate up to the second order. There are known applications of this method in several areas but very few in processes involving the production of polymers.[15,16] However, the conventional UKF presents potential disadvantages such as the disregard of bounds and other constraints on parameters and state variables. It has been shown that these may lead to poor filter performance under some circumstances. Consequently modifications that improve its performance were developed, such as the Unscented Recursive Nonlinear Dynamic Data Reconciliation (URNDDR)[17] and the Reformulated Constrained Unscented Kalman Filter (RCUKF).[18] These variants incorporate the possibility of adding constraints on the estimated states.

The process measurements that are available for estimation purposes are usually of the following types: continuous measurements which can be obtained at high sampling frequency, delayed measurements from different devices that are available at a fixed sampling rate, and manual laboratory measurements which are available at unequal intervals and with varying delays.[19] Very few works related to state estimation in control systems refer to

the use of delayed measurements and how they affect the quality of the estimate.

In polymer processes, in particular, several critical quality variables belong to the last two types of aforementioned observations. For instance, the polymer MWD and its averages, which can be measured by either online or offline size exclusion chromatography (SEC). In the case of offline equipments, the measurement delay is usually of 60 min or more. When using online devices, there is still a hold-up time for sample preparation and separation of ≈15 min when using a single SEC column, or longer if more columns are used for a more efficient separation.[5,20]

Therefore, delayed values of these molecular properties have to be incorporated to the estimation scheme to enhance process knowledge. In state estimation problems using MHE, this type of measurement is easily treated, but in general and depending on how large the data window is, these methods have a high computational cost. Regarding filtering estimation techniques, different procedures are available for dealing with delayed measurements. One of them consists in modifying the structure of the filtering algorithm, but a general method is not available due to its intrinsic complexity. Only applications to linear cases and some specific cases of non-linear filters have been reported up to the present time.[21,22] Another way is to develop an estimation procedure which identifies when delayed observations are available and performs a re-estimation of the states.[20] The literature provides some case studies of polymerization processes that take into account delayed measurements using EKF with this re-estimation loop.[7,19,23]. Also the procedure developed by Mutha et al.,[24] which is based on an EKF with fixed-lag smoothing, can be applied.

This work aims at using filtering strategies based on the UT into an estimation scheme that deals with delayed measurements, focusing on applications to polymer processes. The conventional UKF and two of its potential improvements, the URNDDR and the RCUKF, are selected as filtering techniques. The performances of the estimation procedures are evaluated in terms of appropriate parameters, which indicate their likely behavior in control systems and real-time optimization procedures.

The rest of the paper is organized as follows. In the next section, the nonlinear state estimation problem is formulated, and the estimation scheme to deal with delayed measurements is explained. Next, two case studies from the literature are briefly reviewed and the application results of the estimation strategies to these processes are presented and discussed.

Nonlinear State Estimation Using Delayed Measurements

A state-space representation is commonly used for describing physical systems. The approaches that follow will be concerned with batch and continuous polymerization processes described by a set of ordinary differential equations. The operation of these continuous time nonlinear systems can be written as

$$\frac{d\mathbf{x}}{dt} = f(\mathbf{x}, \mathbf{u}, t) + \mathbf{w}(t), \quad \mathbf{w}(t) \sim N[0, \mathbf{Q}(t)] \tag{1}$$

where $\mathbf{x}$ is the n-dimensional state vector, $f(\mathbf{x},\mathbf{u},t)$ the n-dimensional vector-valued function, $\mathbf{u}$ represents the vector of known manipulated inputs, and $\mathbf{w}(t)$ stands for the n-dimensional process noise vector with covariance $\mathbf{Q}(t)$.

At discrete instants of time the following m-dimensional observation vector $\mathbf{y}_k$ is obtained

$$\mathbf{y}_k = h(\mathbf{x}_k) + \mathbf{v}_k, \quad \mathbf{v}_k \sim N[0, \mathbf{R}_k] \tag{2}$$

where h is the measurement equation and $\mathbf{v}_k$ represents the m-dimensional observation noise vector with covariance $\mathbf{R}_k$. The vectors $\mathbf{v}$ and $\mathbf{w}$ are zero mean white Gaussian noise assumed to be independent of each other.

When the value of a delayed measurement is available, the following measurement equation replaces Equation 2,

$$\mathbf{y}^{\mathrm{d}}_{k-\tau} = h_{\mathrm{d}}\left(\mathbf{x}^{\mathrm{d}}_{k-\tau}\right) + \mathbf{v}^{\mathrm{d}}_{k-\tau}, \quad \mathbf{v}^{\mathrm{d}}_{k-\tau} \sim N\left[0, \mathbf{R}^{\mathrm{d}}_{k-\tau}\right] \tag{3}$$

The dimensions of matrices $\mathbf{R}^{\mathrm{d}}_{k-\tau}$ and $\mathbf{R}_k$ depend on the number of variables measured at the corresponding time, and τ represents the time intervals elapsed since the delayed measurement was obtained.

In Figure 1 a typical flow diagram of a state estimation process is shown.

In any state estimation technique, observability is a primary issue. A system is completely observable if every initial state can be determined through knowledge of the manipulated variables and system outputs over some finite time interval.[25]

As mentioned before, different approaches have been proposed in the literature to adapt existing estimation methods in order to incorporate information from delayed measurements. One of these is the so-called two-timescale estimation technique. This approach does not require modifying the basic algorithm of the filter. Instead, it incorporates information of delayed measurements by

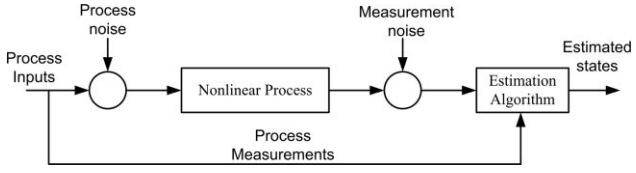

Figure 1. General state estimation.

recalculating past trajectories. This method has been applied successfully to the EKF.[7,19,23] In this work, we analyze the performance of this technique for three filters of the UT family: the conventional UKF and two of its variants, the URNDDR and the RCUKF. The standard algorithms for online measurements corresponding to these filters are shown in the Appendix. The application of the two-timescale technique is explained below.

The standard procedures of the aforementioned filters consist of two stages: a stage of propagation of states through the model and a stage of update of the states against measurement values. The first one takes place between online sampling times. In this stage, the filter yields predicted values of the states $\hat{x}_k^-$, $(t_{k-1} \leq t \leq t_k)$, by solving the process model using the information available up to the time t_{k-1}. The update stage takes place at sampling intervals k, when state updates $\hat{x}_k^+$ are obtained by correcting the predicted values $\hat{x}_k^-$ against the online measurements y_k^0. The updated values $\hat{x}_k^+$ are then the starting points for the next propagation stage.

In the two-timescale filter, the estimation operates like in its standard counterpart meanwhile delayed measurements are not available. However, predicted states and online measurements trajectories $\hat{x}_k^-$ and y^0 are stored. When a delayed measurement $y_{k-\tau}^d$, corresponding to a past time interval $(k-\tau)$, arrives at the current time t_k, firstly the past predicted states $\hat{x}_{k-\tau}^-$ are re-updated against the stored online measurements $y_{k-\tau}^0$ but also against the delayed measurements $y_{k-\tau}^d$, obtaining a new $\hat{x}_{k-\tau}^+$. Using this value as starting point, the trajectory between $t_{k-\tau}$ and t_k is then recalculated. This involves repetition of the propagation and online updates in the period $[t_{k-\tau}, t_k]$. In this way the updated states $\hat{x}_k^+$ are obtained that are the initial points for the next propagation stage of the filter.

In the next section, the performance of the two-timescale UT filters is analyzed with two case studies of polymer processes of different complexity.

Case Studies

Two case studies of different mathematical complexity, taken from the literature, were used to evaluate the performances of the two-timescale UKF, URNDDR, and RCUKF filters. The first case study is a styrene solution polymerization in a continuous stirred-tank reactor (CSTR).[26] In this case the mathematical model is simple, involving six state variables which include reactant concentrations and average molecular weights of the polymer. Two online measurements and two delayed measurements are considered. The second case study involves a solution copolymerization reactor with recycle.[27] The mathematical model of this process presents an increased complexity, involving 24 states and several algebraic nonlinear equations. The model predicts conversion and copolymer average molecular weights and composition. In this case three online measurements and two delayed measurements are considered. Details of the two case studies are presented below.

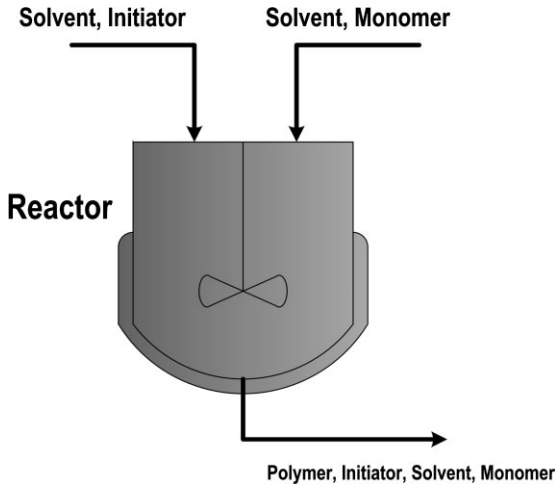

Figure 2. Styrene solution polymerization reactor.

Case 1: Styrene Polymerization

This process is a solution styrene polymerization in a CSTR, in which toluene is used as solvent and azoisobutyronitrile (AIBN) as initiator. A diagram of the polymerization reactor is shown in Figure 2. The reactor feed consists of two streams; one of them is a solution of initiator in toluene, and the other one a solution of styrene in the same solvent. Polystyrene, unreacted monomer, solvent and initiator, compose the exit stream. The reactor temperature is tightly controlled independently of other process conditions.[26]

The mathematical model is based on the following kinetic steps: initiation, propagation, transfer to monomer, and solvent and termination by combination. Under the operating conditions studied in this case, the gel and glass effects are negligible.[28] The balance equations of the model are the following.

Initiator:

$$\frac{dC_I}{dt} = -\left(\frac{F_T}{V} + k_i\right) C_I + \frac{F_1 C_{I,1}}{V} \tag{4}$$

Solvent:

$$\frac{dC_S}{dt} = -\frac{F_T C_S}{V} + \frac{F_T C_{S,1} + F_2 C_{S,2}}{V} \tag{5}$$

Monomer:

$$\frac{dC_M}{dt} = -k_p C_M P + \frac{F_2 C_{M,2} - F_T C_M}{V} \quad (6)$$

First-Order Moment of the Polymer MWD:

$$\frac{d\lambda_1}{dt} = -\frac{F_T \lambda_1}{V} + [(k_{fm} C_M + k_{td} P + k_{fs} C_S)(2\alpha - \alpha^2) + k_{tc} P] \frac{P}{(1-\alpha)} \quad (7)$$

Number-Average Molecular Weight:

$$\frac{d\overline{M}_n}{dt} = \left\{ \begin{array}{c} [(k_{fm} C_M + k_{td} P + k_{fs} C_S)(2\alpha - \alpha^2) + k_{tc} P] \\ -[(k_{fm} C_M + k_{td} P + k_{fs} C_S)\alpha + 0.5 k_{tc} P] \frac{\overline{M}_n}{M_M}(1-\alpha) \end{array} \right\} \frac{P\overline{M}_n}{\lambda_1(1-\alpha)} \quad (8)$$

Weight-Average Molecular Weight:

$$\frac{d\overline{M}_w}{dt} = \left\{ \begin{array}{c} [(k_{fm} C_M + k_{td} P + k_{fs} C_S)(\alpha^3 - 3\alpha^2 + 4\alpha) + k_{tc} P(\alpha + 2)] \\ -[(k_{fm} C_M + k_{td} P + k_{fs} C_S)(2\alpha - \alpha^2) + k_{tc} P] \frac{\overline{M}_w}{M_M}(1-\alpha) \end{array} \right\} \frac{P M_M}{\lambda_1 (1-\alpha)^2} \quad (9)$$

where

$$\alpha = \frac{k_p C_M}{(k_p + k_{fm}) C_M + k_{fs} C_S + k_t P} \quad (10)$$

Besides, the total radical concentration is

$$P = \sqrt{\frac{2 f C_I k_i}{k_t}} \quad (11)$$

and the volumetric flow rate of the outlet stream is

$$F_T = F_1 + F_2 \quad (12)$$

As the reactor temperature is kept tightly around its desired value by its control system, the energy balance is not included. The kinetic constants used above are

$$k_i = 0.693 \Big/ \left(60 \times 10^{((A_i/T)+B_i)}\right) \quad (13)$$

$$k_p = A_p e^{-\frac{E_p}{RT}} \quad (14)$$

$$k_{fm} = A_{fm} e^{-\frac{E_{fm}}{RT}} \quad (15)$$

$$k_{fs} = A_{fs} e^{-\frac{E_{fs}}{RT}} \quad (16)$$

$$k_t = A_t e^{-\frac{E_t}{RT}} \quad (17)$$

$$k_{td} = 0.15 \times k_t \quad (18)$$

$$k_{tc} = 0.85 \times k_t \quad (19)$$

In the previous equations, C_j is the molar concentration of species j; F_1 and F_2 are the volumetric flow rates of the initiator solution stream and the monomer solution stream, respectively, f the initiator efficiency, M_M styrene molecular weight, and V is the reactor volume. This model has been validated experimentally. The values of the model parameters are found in the literature.[26]

For the analysis of the proposed filters, it is considered that the initiator concentration C_I and the monomer concentration C_M are measured online with a sampling interval of 5 min,[5] while the number-average molecular weight $\overline{M}_n$ and the weight-average molecular weight $\overline{M}_w$ are delayed measurements with a certain delay time.

Case 2: MMA – Vinyl Acetate Copolymerization

The process selected as second case study is a solution polymerization in a CSTR with a recycle loop. This is a system that has been chosen in several works dealing with state estimation and process control applications.[27,29] Figure 3 shows a diagram of the reactor. The comonomers, MMA and vinyl acetate (VA) are continuously added, together with AIBN as initiator, benzene (B) as solvent and acetaldehyde as chain transfer agent (CTA). The monomer stream may also contain inhibitors such as *m*-dinitrobenzene. These are the components of the fresh feed stream (F_1). This is combined with the recycle stream (F_2) to form the reactor feed stream (F_3). Polymer, solvent, unreacted monomers, initiator, and CTA flow out of reactor to a separator (F_4), from which unreacted monomers and solvent continue to the purge point (F_7). After the purge (F_9) they are stored in a recycle hold tank.

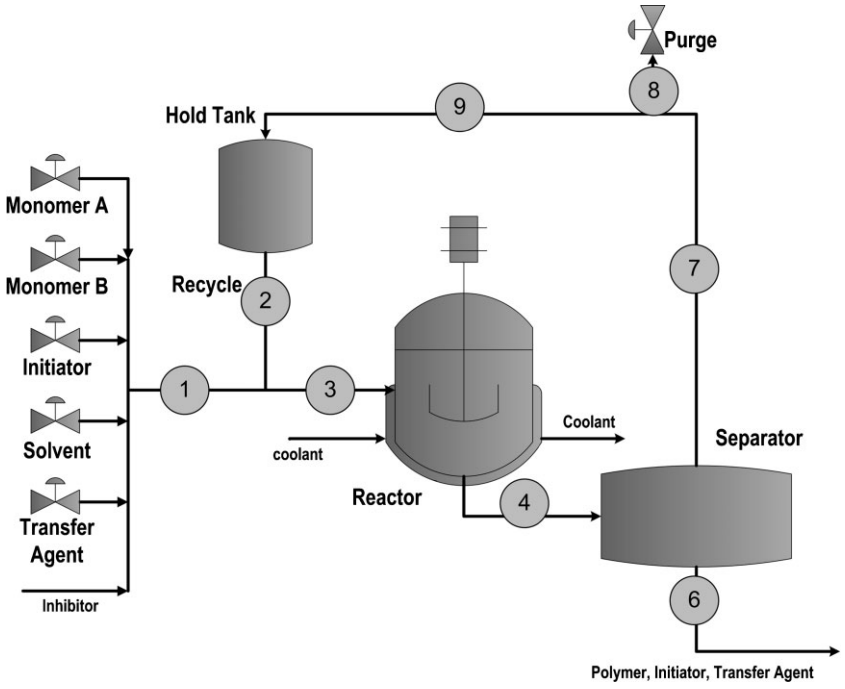

Figure 3. Copolymerization reactor.

This system is represented by a first principles model consisting of a set of differential algebraic equations (DAE), whose most important equations are:

Reactor Mass and Moment Balances:

$$\frac{dC_k}{dt} = \frac{C_{k,f} - C_k}{\theta_r} + R_k \qquad C_k(0) = C_{k,0} \quad k = \text{MMA, VA, AIBN, } B\text{, CTA, inh} \tag{20}$$

$$\frac{d\lambda_k}{dt} = \frac{\lambda_{k,f} - \lambda_k}{\theta_r} + S_k \quad \lambda_k(0) = \lambda_{k,0} \qquad k = \text{MMA, VA} \tag{21}$$

$$\frac{d\psi_k}{dt} = \frac{\psi_{k,f} - \psi_k}{\theta_r} + T_k \quad \psi_k(0) = \psi_{k,0}\ k = 0, 1, 2 \tag{22}$$

where subscript f stands for feed stream, C_k the molar concentration of species k and λ_k the molar concentration of monomer k in the copolymer, ψ_k the kth-order moment of the copolymer MWD, θ_r is the residence time of reactor, and R_k, S_k, and T_k are reaction rates.

Reactor Energy Balance:

$$\frac{dT_r}{dt} = \frac{T_{r,f} - T_r}{\theta_r} + \frac{(-\Delta H_{paa}) k_{paa} C_{MMA} C^*_{MMA} + (-\Delta H_{pba}) k_{pba} C_{MMA} C^*_{VA}}{\rho_r c_{p,r}} + \frac{(-\Delta H_{pab}) k_{pab} C_{VA} C^*_{MMA} + (-\Delta H_{pbb}) k_{pbb} C_{VA} C^*_{VA}}{\rho_r c_{p,r}} - \frac{U_r S_r (T_r - T_j)}{V \rho_r c_{p,r}}, \qquad T_r(0) = T_{r,0} \tag{23}$$

where C^*_{MMA} and C^*_{VA} denote the global concentration of radicals with a MMA and a VA terminal unit, respectively, ρ_r and $c_{p,r}$ represent the density and heat-capacity of the reaction mixture, respectively, ΔH_{paa}, ΔH_{pba}, ΔH_{pab} and ΔH_{pbb} are reaction enthalpies, and k_{paa}, k_{pba}, k_{pab} and k_{pbb} are kinetic constants, of the propagation reactions; U_r and S_r are the overall heat-transfer coefficient and transfer area, respectively, and T_j is the temperature of the reactor jacket.

Separator Balances:

$$\frac{dC_{k,s}}{dt} = \frac{C_{k,s,f} - \frac{F_n}{F_4} C_{k,s}}{\theta_s}, \qquad C_{k,s}(0) = C_{k,s,0}, \qquad k = \text{MMA, VA, AIBN, B, CTA, inh} \tag{24}$$

where θ_s is the residence time in the separator and $n = 7$ for $k =$ AIBN, CTA, inh, and $n = 6$ for $k =$ MMA, VA, B.

Hold Tank Balances:

$$\frac{dC_{k,h}}{dt} = \frac{C_{k,h,f} - C_{k,h}}{\theta_h}, \qquad C_{k,h}(0) = C_{k,h,0}, \quad k = \text{MMA, VA, B} \tag{25}$$

where θ_h is the residence time in the hold tank.

Average Molecular Weights, Composition and Conversion:

$$\overline{M}_n = \frac{\psi_1}{\psi_0} \tag{26}$$

$$\overline{M}_w = \frac{\psi_2}{\psi_1} \tag{27}$$

$$Y_{MMA} = \frac{\lambda_{MMA}}{\lambda_{MMA} + \lambda_{VA}} \tag{28}$$

$$\text{Conv} = \frac{\psi_1}{(\psi_1 + M_{MMA} C_{MMA} + M_{VA} C_{VA})} \tag{29}$$

where Y_{MMA} is the number-average composition of MMA in the copolymer and M_{MMA} and M_{VA} are the molecular weights of MMA and VA, respectively. This mathematical

model is supported by experimental validation. More details on the model equations, such as algebraic equations for stream connections, reaction rates, global concentration of radicals, and parameters can be found in ref.[27]

For this case study, it is considered that the reactor temperature T_r, the total conversion Conv and the copolymer composition Y_{MMA} are measured online with a sampling interval of 5 min,[5] while the number-average molecular weight $\overline{M}_n$ and the weight-average molecular weight $\overline{M}_w$ are delayed measurements with a certain delay time.

Table 1. Base case operating point for Case I.

Variable	Value	Unit
T	393	K
F_1	1.54×10^{-4}	kmol s^{-1}
F_2	1.54×10^{-4}	kmol s^{-1}
$C_{M,2}$	6.38×10^{6}	kmol m^{-3}
$C_{I,1}$	0.1138	kmol m^{-3}
$C_{S,i}$	9.2	kmol m^{-3}
$C_{S,2}$	1.75	kmol m^{-3}
V	0.48	m^3

Results and Discussion

Different tests were carried out in order to analyze the performance of two-timescale filtering techniques. Furthermore the behavior of a multirate EKF[9] (MEKF) technique was studied. In these tests, measurement white noise ($\mathbf{v}_k$) was modeled by corrupting the actual measurement values given by the solution of the DAE system ($h(\mathbf{x}_k)$), with a pseudo random number generator. The perturbation was set to be within three standard deviations of the true values. The elements of the observation noise covariance matrix $\mathbf{R}$ were set in agreement with typical instrumentation of polymer reactors. The elements of the process noise covariance matrix $\mathbf{Q}$ were tuned by trial and error in order to improve convergence of the filter. Finally, the initial values of the error covariance matrix $\mathbf{P}_0$ were set as the ones resulting of preliminary filter runs. The filter algorithms were implemented in Matlab with an embedded process model developed in gPROMS. Besides, Matlab was linked to GAMS for carrying out the solution of the optimization problems in the update steps of the URNDDR and RCUKF filters. A PC equipped with a Pentium 4 (3 GHz) processor and 2 GB RAM was employed.

The three UT filters analyzed in this work proved to be successful in the estimation of all process variables. However, since this work focuses on the handling of delayed measurements with the UT filters, results will be presented for the estimation of the number and weight-average molecular weights. In the first case study, measured variables were the initiator and monomer concentrations and the number and weight-average molecular weights. The first two were considered to be measured online with a sampling interval of 5 min, while average molecular weight data were received with a certain delay. Several dynamic scenarios were simulated by perturbation of a base-case operating point. This corresponds to a steady-state point defined by the operating conditions shown in Table 1. Results are presented for one of these scenarios selected as example. In this scenario, a step change in the initiator flow rate F_1 is made at time 1 h, from an initial value of 1.54×10^{-4} kmol s^{-1} to a final value of 7.9×10^{-5} kmol s^{-1}. The process was sampled 100 times in all tests.

Figure 4 shows the results of the estimation of $\overline{M}_w$ for different measurement delays, for the three UT filters. Besides, estimation with a classical two-timescale EKF[20] and the MEKF technique were included for comparison. This plot corresponds to one of the 100 process samples. Initial estimates of the states were set in order to start with an initial error of 10% in $\overline{M}_w$, while the remaining variables were initialized at their actual values. It can be seen that convergence is achieved in similar times for all filters in each situation. However, the UT filters outperform the EKF and MEKF in terms of smoothness of the estimated trajectories and error with respect to the actual values. The difference in performance becomes more noticeable as the delay time increases and the filter is more seriously challenged. On the other hand, the behaviors of the three UT filters are very similar to each other.

It can also be seen that convergence time increases with delay time. In the case of a 15 min delay, convergence is achieved in ≈1 h; however, it takes nearly 4 h for a delay of 45 min. This is an expected result because the system is not observable when molecular weights measurements are not available. Hence, at longer measurement delays state prediction is carried out under non-observability conditions for a longer period of time, and thus the estimates become more deficient. The filters' performances for the random measurement delay are in an intermediate position between the ones with fixed delays. This behavior for different delay times are in agreement with previous studies on two-timescale EKF filters.[20] Similar results were obtained for $\overline{M}_n$ as shown in Figure 5.

Figure 6 shows the comparative values of the average root square error (ARSE) over the 100 process samples corresponding to the different filters for the delay periods analyzed. In this figure it is possible to see that the ARSE is smaller for the UT filters than for the EKF and the MEKF, with a slight superiority of the RCUKF and the URNDDR over

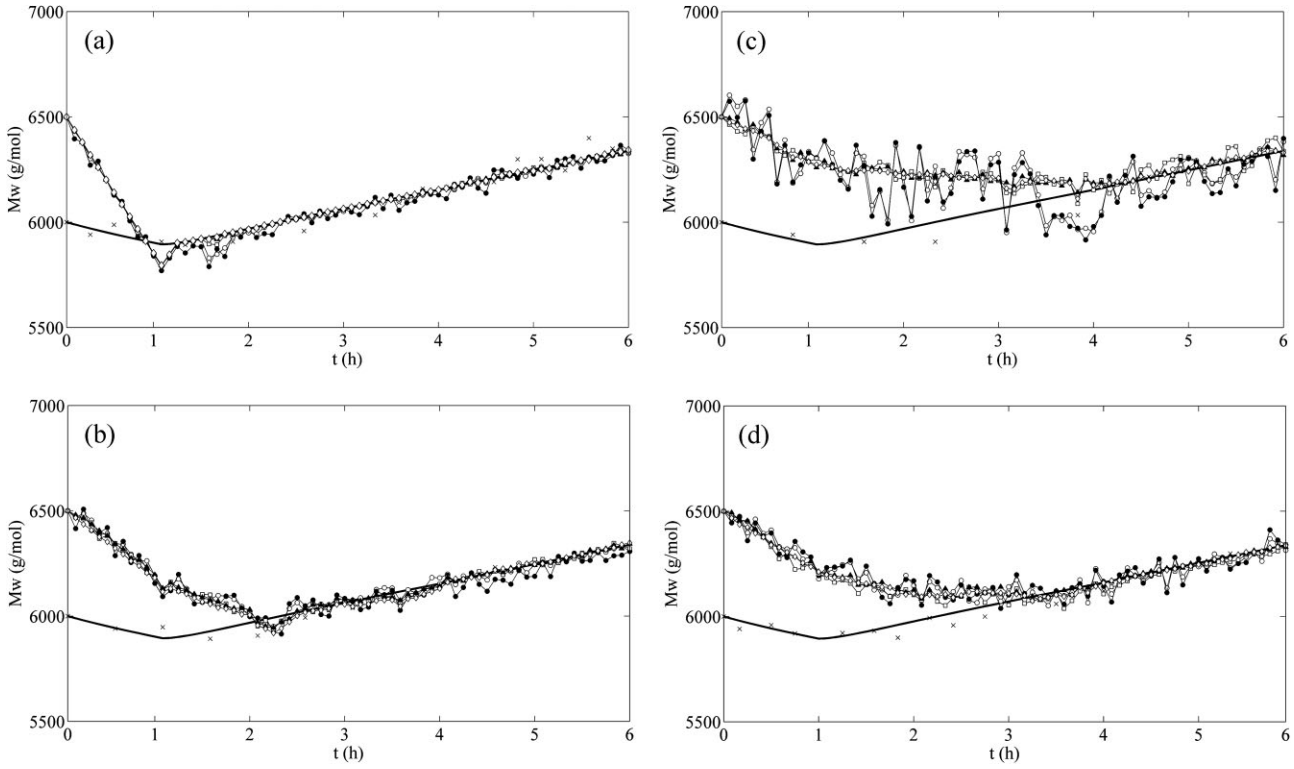

Figure 4. Estimation of $\overline{M}_w$ for (a) 15 min, (b) 30 min, (c) 45 min (d) and random measurement (between 15 and 45 min) delay for Case I. — True value; × measurements: —○— EKF; —●— MEKF; —□— UKF; —▲— URNDDR; —◇— RCUKF.

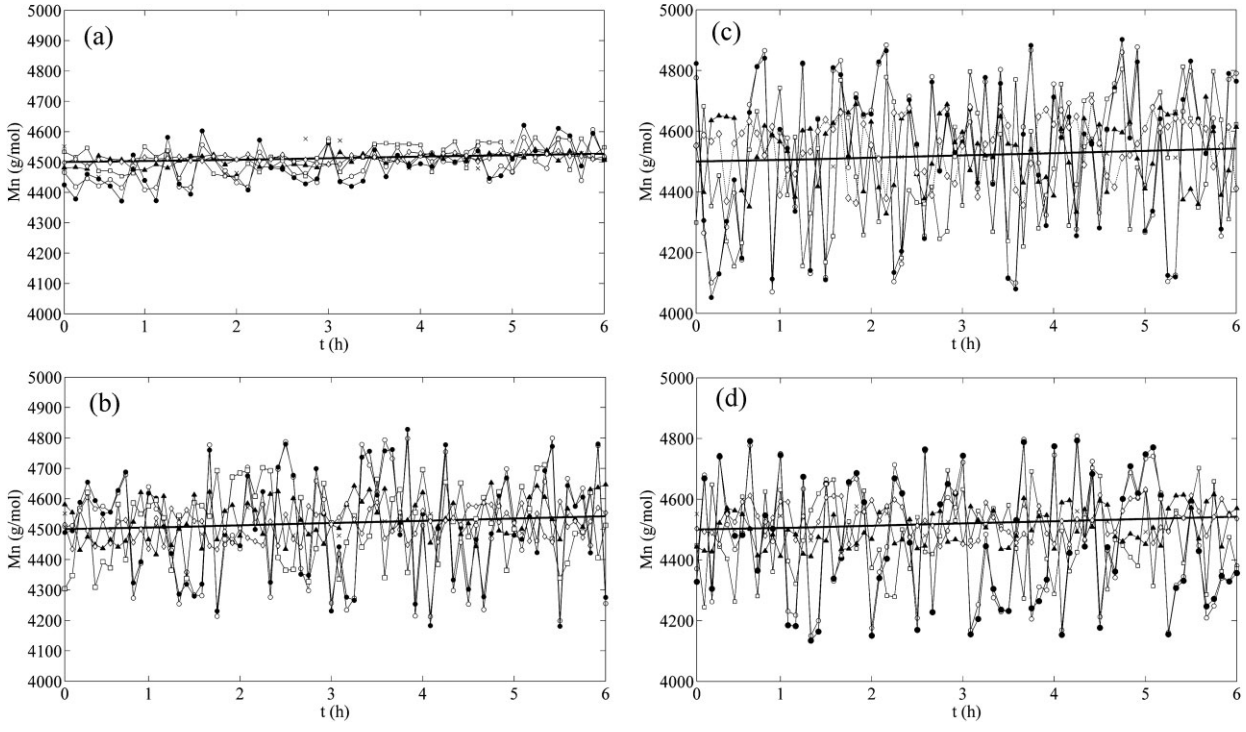

Figure 5. Estimation of $\overline{M}_n$ for (a) 15 min, (b) 30 min, (c) 45 min (d) and random measurement (between 15 and 45 min) delay for Case I. — True value; × measurements: —○—EKF; —●— MEKF; —□— UKF; —▲— URNDDR; —◇— RCUKF.

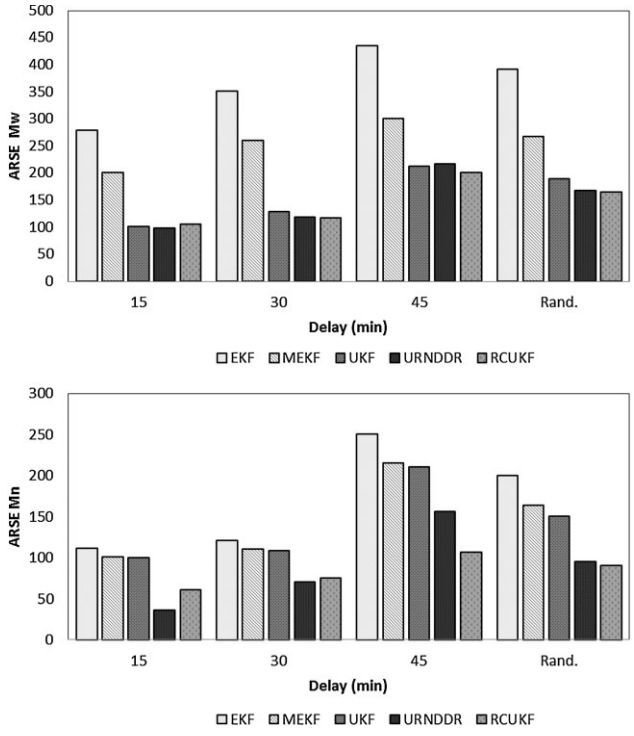

Figure 6. Average root square error for $\overline{M}_w$ and $\overline{M}_n$ in Case I.

the classical UKF, especially for the variable with an error in the initial condition. It can also be observed that when the measurements are randomly delayed between 15 and 45 min, the error is between the ones for the fixed 15 min and the fixed 45 min delays, which confirms the previous observation in Figure 4 about this point.

In the second case study, the reactor temperature, the total conversion, and the copolymer composition were regarded as online measurements with a sampling time of 5 min. Number and weight-average molecular weights measurements were received with a certain delay. As in the previous case, several dynamic scenarios were simulated and one of them was selected as example to show the results of the analysis of the filters' performances. In the chosen example, time 0 corresponds to an intermediate point during a transition toward a new steady state. Relevant process variables for this scenario are presented in Table 2 and 3. The process was sampled 100 times in all tests.

Table 2. Operating conditions for Case II.

Parameter	Value	Unit
F_3	9.35	kmol s^{-1}
$C_{MMA,f}$	5.15	kmol m^{-3}
$C_{VA,f}$	2.97	kmol m^{-3}
$C_{AIBN,f}$	4.6×10^{-3}	kmol m^{-3}
$C_{B,f}$	1.31	kmol m^{-3}
$C_{CTA,f}$	1.17	kmol m^{-3}
$C_{inh,f}$	0	kmol m^{-3}
T_j	336	K
$T_{r,f}$	353	K
purge fraction	0.05	
V_r	1	m^3
S_r	4.6	m^2

Similarly to Case I, Figure 7 and 8 show the estimation of $\overline{M}_w$ and $\overline{M}_n$ for one of the 100 process samples of the selected scenario. It should be noted that in Case II the estimation is initialized at a transition point of the system, which increases the possibility of inaccuracy. The initial values were taken with an error of 10%. A similar pattern in

Table 3. Initial conditions for Case II.

State	Value	Unit	State	Value	Unit
$C_{MMA,0}$	1.83	kmol m^{-3}	$C_{MMA,s,0}$	1.83	kmol m^{-3}
$C_{VA,0}$	3.38	kmol m^{-3}	$C_{VA,s,0}$	3.38	kmol m^{-3}
$C_{AIBN,0}$	1.22×10^{-4}	kmol m^{-3}	$C_{AIBN,s,0}$	1.22×10^{-4}	kmol m^{-3}
$C_{B,0}$	1.65	kmol m^{-3}	$C_{B,s,0}$	1.65	kmol m^{-3}
$C_{CTA,0}$	0.22	kmol m^{-3}	$C_{CTA,s,0}$	0.25	kmol m^{-3}
$C_{inh,0}$	0	kmol m^{-3}	$C_{inh,s,0}$	0	kmol m^{-3}
$T_{r,0}$	3822	K	$C_{MMA,h,0}$	2.035	kmol m^{-3}
$\lambda_{MMA,0}$	2.54	kmol m^{-3}	$C_{VA,h,0}$	3.76	kmol m^{-3}
$\lambda_{VA,0}$	0.36	kmol m^{-3}	$C_{AIBN,h,0}$	0	kmol m^{-3}
$\psi_{0,0}$	5.63×10^{-3}	kmol m^{-3}	$C_{B,h,0}$	1.83	kmol m^{-3}
$\psi_{1,0}$	256.09	kg m^{-3}	$C_{CTA,h,0}$	0	kmol m^{-3}
$\psi_{2,0}$	2.1×10^6	kg^2 $kmol^{-1}$ m^{-3}	$C_{inh,h,0}$	0	kmol m^{-3}

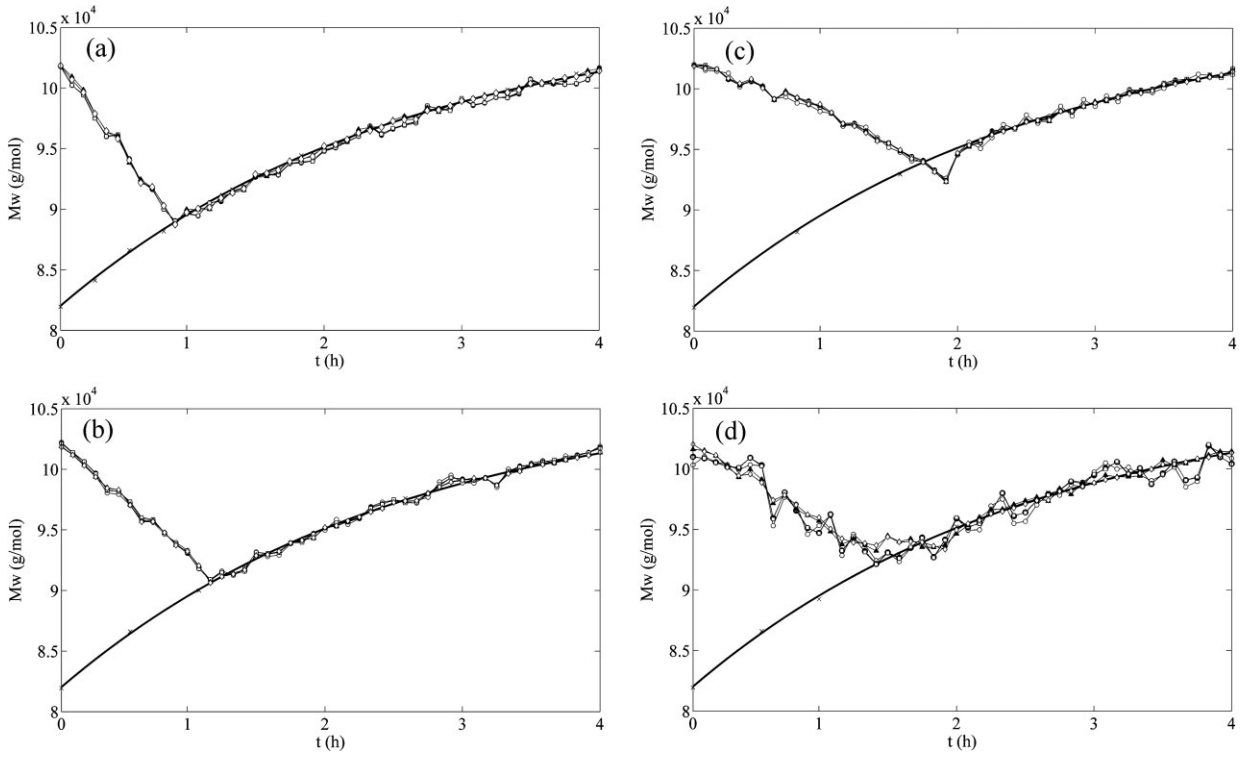

Figure 7. Estimation of $\overline{M}_w$ for (a) 15 min, (b) 30 min, (c) 45 min (d) and random measurement (between 15 and 45 min) delay for Case II. — True value; × measurements: —○— EKF; —●— MEKF; —□— UKF; —▲— URNDDR; —◇— RCUKF.

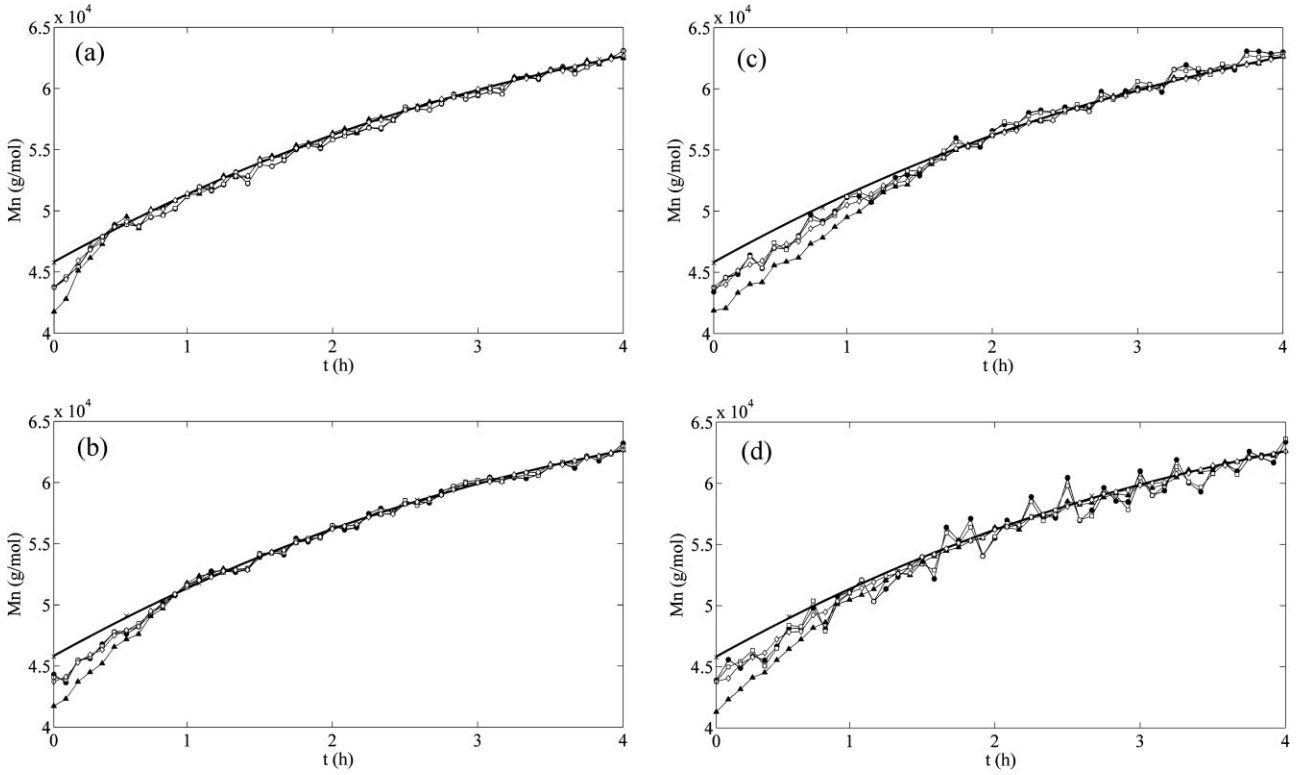

Figure 8. Estimation of $\overline{M}_n$ for (a) 15 min, (b) 30 min, (c) 45 min (d) and random measurement (between 15 and 45 min) delay for Case II. — True value; × measurements: —○— EKF; —●— MEKF; —□— UKF; —▲— URNDDR; —◇— RCUKF.

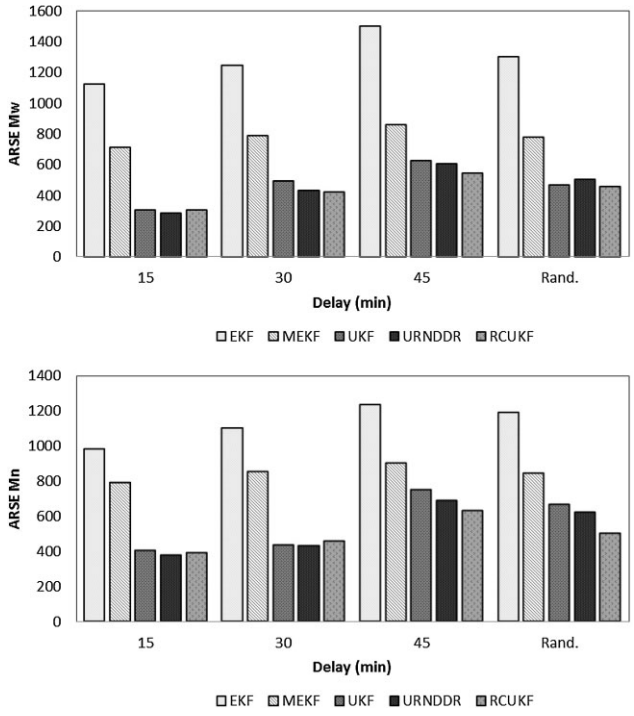

Figure 9. Average root square error for $\overline{M}_w$ and $\overline{M}_n$ in Case II.

Table 4. Computational times of the different filters for Case I.

Step	EKF [s]	MEKF [s]	UKF [s]	URNDDR [s]	RCUKF [s]
propagation	0.48	0.51	1.13	1.63	1.18
update	0.71	0.84	0.213	5.53	6.56
delay – 15 min	5.24	4.26	6.49	30.29	32.13
delay – 30 min	12.43	8.32	9.83	49.45	47.77
delay – 45 min	19.48	13.5	17.97	68.50	70.90

Table 5. Computational times of the different filters for Case II.

Step	EKF [s]	MEKF [s]	UKF [s]	URNDDR [s]	RCUKF [s]
propagation	2.90	3.2	6.77	9.79	7.08
update	4.23	3.98	1.28	33.20	39.35
delay – 15 min	39.43	17.21	38.93	192.73	202.79
delay – 30 min	57.85	29.65	56.97	254.72	240.28
delay – 45 min	99.77	48.32	87.86	391.90	385.58

convergence time and accuracy in the estimation than in Case I can be observed. Even though the number of states is significantly higher and the process dynamics is more complex, the UT filters show a very good performance, with superior results than the EKF and the MEKF. This is confirmed by the ARSE values presented in Figure 9.

Another critical aspect in a filter performance is the computational time. The time required by the filter to provide estimate values is extremely important in the subsequent stages of control and online optimization. This feature was analyzed for each of the filters studied in this work. The average computational time over the 100 process samples was evaluated for Cases I and II, distinguishing between the individual steps of propagation, update and reestimation that compose the UKF filters' algorithms. The resulting values are presented in Table 4 and 5. It can be observed that the lowest values among the two-timescale filters correspond to the EKF and the UKF. These filters show comparable CPU time requirements. The sum of propagation and update times are similar, and therefore so is the reestimation time, which involves repetition of propagation and update steps from time $t_{(k-\tau)}$ to time t_k. Since its processing time is only of a few seconds, the UKF turns out to be an attractive option for online applications.

The URNDDR and the RCUKF, on the other hand, present a considerably higher time requirement. It can be seen that the most time consuming step is the update step. Unlike the conventional UKF, in the URNDDR and the RCUKF this step involves solving an optimization problem. Solution of optimization problems require larger times than the pure algebraic operations performed in the UKF, and hence the CPU time increases. Because of this, the reestimation time is markedly higher than for the UKF. In Case I, where the model involves only six states, the reestimation time reaches up to about a 20% of the online sampling time of 5 min. However, in Case II that involves 24 states, the reestimation time can be up to 30% greater than the online sampling time, meaning that the estimate of the states will not be available before the arrival of new measurements. The main potential advantages of the URNDDR and the RCUKF over the conventional UKF are their capability of handling constraints. However, no situations of failure of the UKF due to the absence of constraints, such as concentrations' estimates yielding negative values, were encountered in this work.

Regarding MEKF, the average computational time over the 100 process samples was also evaluated for Cases I and II, distinguishing between the individual steps of propagation, update, and estimation of the new state values by smoothing. Results are included in Table 4 and 5. The smoothing interval was established as suggested by Muhta et al.[24] It can be noticed that the lowest computational time for all the analyzed techniques corresponds to MEKF. This is due to the fact that the two-timescale procedure involves a re-estimation step that uses original filters algorithms; in contrast, MEKF employs a modification of the standard EKF algorithm and does not recalculate past trajectories.

Conclusion

A two-timescale method was applied to the UKF, the URNDDR and the RCUKF filters in order to incorporate delayed measurements into their estimation scheme. A thorough analysis on the performance of these filters in two case studies involving polymer processes showed that these filters have excellent convergence and accuracy properties, outperforming the standard EKF and MEKF.

It was found that the delay time in the acquisition of the measurement data influences the filters' performances. Longer delays caused longer convergence times and deterioration of the filter accuracy, which is in agreement with reported results on two-timescale EKFs.

The three UT filters presented similar convergence and accuracy properties. However, the UKF required much less computational time, which makes it the most attractive alternative for online state estimation for processes like the ones studied in this work. This difference in computational requirement comes from the optimization problem that is performed in the update step of the URNDDR and the RCUKF, in contrast to the direct vector-matrix operations involved in the UKF.

No failure due to absence of constraints in the UKF was detected for the processes studied in this work, making futile the main advantages of the URNDDR and the RCUKF over the UKF.

Appendix

This appendix includes the standard algorithms of the EKF and the UT filters UKF, URNDDR and RCUKF, for the state estimation with online measurements.

Extended Kalman Filter

One of the most common ways to solve the problem of state estimation from disturbed measurement variables is the EKF. Table A.1 shows the algorithm employed in several texts.[25,30]

EKF with Fixed-Lag Smoothing for Multirate Systems

The MEKF is based on a "boop-strap" application of filtering and smoothing. Two EKF algorithms are used in this scheme: one for filtering the states when only online measurements are available, and the second for smoothing the states when delayed measurements arrive. This procedure was developed by Mutha et al.[24] The algorithm is shown in Table A.2.

Unscented Filters Family Equation Section (Next)

Estimation algorithms like the EKF, based on Gaussian noise, may not be applicable to nonlinear systems since Gaussian noise propagated through a nonlinear model is distorted. Besides, severe nonlinearities may prevent the use of theory based on linearization due to poor estimation accuracy. Furthermore, the nonlinear system may have a skew or multimodal probability density function.

The UT is a method for calculating the statistics of a random variable that undergoes a nonlinear transformation.[31] Let $\mathbf{x}$ be an n-dimensional random variable which is propagated through a nonlinear function. It is assumed that $\mathbf{x}$ has mean $\overline{\mathrm{x}}$ and covariance $\mathbf{P_x}$. In order to calculate the statistics of a dependent variable in a nonlinear function, a matrix $\boldsymbol{\chi}$ of $2n+1$ sigma vectors $\boldsymbol{\chi_i}$ is constructed as follows:

$$\chi_0 = \overline{\mathrm{x}} \tag{A.1}$$

$$\boldsymbol{\chi}_i = \overline{\mathbf{x}} + \left(\sqrt{(n+\lambda)\mathbf{P_x}}\right)_i, \quad i = 1, \ldots, n \tag{A.2}$$

$$\boldsymbol{\chi}_i = \overline{\mathbf{x}} + \left(\sqrt{(n+\lambda)\mathbf{P_x}}\right)_{i-n}, \quad i = n+1, \ldots, 2n \tag{A.3}$$

$$\lambda = \alpha^2(n+\kappa) - n \tag{A.4}$$

Table A.1. Algorithm of the extended Kalman filter.

Step	Equation
state estimation propagation	$\dot{\hat{\mathrm{x}}}(t) = f[\hat{\mathrm{x}}(t), \mathbf{u}(t)]$
error covariance propagation	$\dot{\mathbf{P}}(t) = \mathbf{F}(t)\mathbf{P}(t)\mathbf{F}^{\mathrm{T}}(t) + \mathbf{Q}(t)$
state estimation update at t_k with on-line measurements	$\hat{\mathbf{x}}_k^+ = \hat{\mathbf{x}}_k^- + \mathbf{K}_k\left[\mathbf{y}_k - h\left(\hat{\mathbf{x}}_k^-\right)\right]$
error covariance update at t_k with on-line measurements	$\mathbf{P}_k^+ = \left[\mathbf{I} - \mathbf{K}_k\mathbf{H}_{0,k}\right]\mathbf{P}_k^-$
gain matrix at t_k with online measurements	$\mathbf{K}_k = \mathbf{P}_k\mathbf{H}_{0,k}^{\mathrm{T}}\left[\mathbf{H}_{0,k}\mathbf{P}_k^-\mathbf{H}_{0,k}^{\mathrm{T}} + \mathrm{R}_{0,k}\right]^{-1}$
	where
	$\mathbf{F}(t) = \left.\frac{\partial f[\mathbf{x}(t), \mathbf{u}(t)]}{\partial \mathbf{x}(t)}\right\|_{\mathrm{x}(t)=\hat{\mathbf{x}}^-}$ and $\mathbf{H}(t) = \left.\frac{\partial h(\mathbf{x}_k)}{\partial \mathbf{x}_k}\right\|_{\mathrm{x}(t)=\hat{\mathbf{x}}^-}$

Table A.2. Algorithm of the MEKF.

Step	Equation
State estimation propagation and update with standard extended Kalman filter for online measurements	$\dot{\hat{\mathbf{x}}}(t) = f[\hat{\mathbf{x}}(t), \mathbf{u}(t)]$
	$\dot{\mathbf{P}}(t) = \mathbf{F}(t)\mathbf{P}(t) + \mathbf{P}(t)\mathbf{F}^T(t) + \mathbf{Q}(t)$
	$\hat{\mathbf{x}}_k^+ = \hat{\mathbf{x}}_k^- + \mathbf{K}_k\left[\mathbf{y}_k - h\{\hat{\mathbf{x}}_k^-\}\right]$
	$\mathbf{P}_\mathbf{k}^+ = \left[\mathbf{I} - \mathbf{K_k}\mathbf{H}_{0,\mathbf{k}}\right]\mathbf{P}_\mathbf{k}^-$
Fixed-lag smoother for delayed measurement	$\hat{\mathbf{x}}_k^+ = \hat{\mathbf{x}}_k^-$
	$\mathbf{K}_{k,0} = \mathbf{K}_k$
	$\mathbf{P}_\mathbf{k}^{0,0} = \mathbf{P}_\mathbf{k}^-$
	$\forall\ i = 1, \ldots,$ SI (smoothing interval)
	$\mathbf{K}_{k,i} = \mathbf{P}_k^{0,i-1}\mathbf{H}^T\left(\mathbf{H}_k\mathbf{P}_k^{0,0}\mathbf{H}_k^T + \mathbf{R}_k\right)^{-1}$
	$\mathbf{P}_k^{i,i} = \mathbf{P}_k^{i-1,i-1} - \mathbf{P}_k^{0,i-1}\mathbf{H}_k^T\mathbf{K}_k^T\mathbf{F}_k^T$
	$\mathbf{P}_k^{0,i} = \mathbf{P}_k^{0,i-1}\left(\mathbf{F}_k - \mathbf{K}_{k,0}\mathbf{H}_k\right)^T$
	$\hat{\mathbf{x}}_{k+1-i}^+ = \hat{\mathbf{x}}_{k+1-i}^- + \mathbf{K}_{k,i}\left[\mathbf{y}_{k+1-i} - \mathbf{h}\{\hat{\mathbf{x}}_{k+1-i}^-\}\right]$

where λ is a scaling parameter and α a constant which determines the spread of the sigma points around the mean value $\overline{\mathbf{x}}$, and is usually set to a small positive value. Besides, κ is a secondary scaling parameter which is usually set to 0, β is used to incorporate prior knowledge of the distribution of $\mathbf{x}$ (for a Gaussian distribution, $\beta = 2$ is optimal), and $\left(\sqrt{(n+\lambda)\mathbf{P}_\mathbf{x}}\right)_i$ is the ith row of the matrix square root, calculated by using a stable numeric algorithm such as the Choleski decomposition.[10,30] The UT determines the mean and covariance of the system output by approximation, using a weighted sample mean and covariance of the posterior sigma points.

Table A.3. Algorithm of the unscented Kalman filter.

Step	Equation
initialization	$\hat{\mathbf{x}}_0 = E[\mathbf{x}_0]; \mathbf{P}_0 = E\left[(\mathbf{x}_0 - \hat{\mathbf{x}}_0 0)(\mathbf{x}_0 - \hat{\mathbf{x}}_0 0)^{\mathrm{T}}\right]$
computation of sigma points	$\chi_k = \left[\hat{\mathbf{x}}_k\hat{\mathbf{x}}_k\mathbf{k} + \left(\sqrt{(n+\lambda)\mathbf{P}_k}\right)_i\hat{\mathbf{x}}_k\mathbf{k} - \left(\sqrt{(n+\lambda)\mathbf{P}_k}\right)_i\right]$
state estimation propagation	$\chi_k^- = \mathbf{F}[\chi_k, \mathbf{u}_k], \quad \hat{\mathbf{x}}_k\mathbf{k} = \sum_{i=0}^{2n} W_i^{\mathrm{m}}\chi_k^-$
error covariance propagation	$\mathbf{P}_k^- = \sum_{i=0}^{2L} W_i^c\left[\chi_{i,k}^- - \hat{\mathbf{x}}_k^-\right]\left[\chi_{i,k}^- - \hat{\mathbf{x}}_k^-\right]^{\mathrm{T}}$
state estimation update at t_k with on-line measurements	$\hat{\mathbf{x}}_k^+ = \hat{\mathbf{x}}_k^- + \mathbf{K}_k\left[\mathbf{y}_k - \hat{\mathbf{y}}_k\right]$
error covariance update at t_k with on-line measurements	$\mathbf{P}_k^+ = \mathbf{P}_k^- - \mathbf{K}\mathbf{P}_{yk,yk}\mathbf{K}^{\mathrm{T}}$
gain matrix at t_k with on-line measurements	$\mathbf{K}_k = \mathbf{P}_{x_k,y_k}\mathbf{P}_{\mathrm{yk,yk}}^{-1}$
	where
	$\mathbf{I}_k = \mathbf{H}\left[\chi_k^-, \mathbf{u}_k\right], \quad \widehat{\mathbf{y}}_k = \sum_{i=0}^{2L} W_i^{\mathrm{m}}\mathbf{I}_{i,k}$
	$\mathbf{P}_{\mathbf{y}_k,\mathbf{y}_k} = \sum_{i=0}^{2L} W_i^c\left[\mathbf{I}_{i,k} - \hat{\mathbf{x}}_k^-\right]\left[\mathbf{I}_{i,k} - \hat{\mathbf{y}}_k\right]^{\mathrm{T}}$
	$\mathbf{P}_{\mathbf{x}_k,\mathbf{y}_k} = \sum_{i=0}^{2L} W_i^c\left[\chi_{i,k}^- - \hat{\mathbf{x}}_k^-\right]\left[\mathbf{I}_{i,k} - \hat{\mathbf{y}}_k\right]^{\mathrm{T}}$

Table A.4. Algorithm of the RCUKF.

Step	Equation
initialization	$\hat{\mathbf{x}}_0 = E[\mathbf{x}_0], \quad \mathbf{P}_0 = E\left[(\mathbf{x}_0 - \hat{\mathbf{x}}_0)(\mathbf{x}_0 - \hat{\mathbf{x}}_0)^{\mathrm{T}}\right]$
computation of sigma points	$\chi_k = \left[\hat{\mathbf{x}}_k \hat{\mathbf{x}}_k + \left(\sqrt{(L+\lambda)}\mathbf{P}_k\right)_i \hat{\mathbf{x}}_k - \left(\sqrt{(L+\lambda)}\mathbf{P}_k\right)_i\right]$
state estimation propagation	$\chi_k^- = \mathbf{F}[\chi_k, \mathbf{u}_k], \quad \hat{\mathbf{x}}_k^- \sum_{i=0}^{2L} W_i^{\mathrm{m}} \chi_k^-$
error covariance propagation	$\mathbf{P}_k^- = \sum_{i=0}^{2L} W_i^{\mathrm{c}} \left[\chi_{i,k}^- - \hat{\mathbf{x}}_k^-\right]\left[\chi_{i,k}^- - \hat{\mathbf{x}}_k^-\right]^{\mathrm{T}}$
state estimation update at t_k with on-line measurements	$\chi_k^+ = \sum_{i=0}^{2L} W_i^{\mathrm{m}} \chi_k^+$
error covariance update at t_k with online measurements	$\mathbf{P}_k^+ = \sum_{i=0}^{2L} W_i \left[\chi_{i,k}^+ - \hat{\mathbf{x}}_k^+\right]\left[\chi_{i,k}^+ - \hat{\mathbf{x}}_k^+\right]^{\mathrm{T}}$
where χ_k^+ is obtained by solving the optimization problem	$\min_{\hat{\chi}_{i,k}^+} \left(\mathbf{y}_k - h\left\{\hat{\chi}_{i,k}^+\right\}\right)^{\mathrm{T}} \mathbf{R}^{-1} \left(\mathbf{y}_k - h\left\{\hat{\chi}_{i,k}^+\right\}\right) + \left(\hat{\chi}_{i,k}^+ - \chi_{i,k}^-\right)^{\mathrm{T}} \left(\mathbf{P}_k^-\right)^{-1} \left(\hat{\chi}_{i,k}^+ - \chi_{i,k}^-\right)$
	$\mathbf{x}_{\mathrm{L}} \le \hat{\chi}_{i,k}^+ \le \mathbf{x}_{\mathrm{U}}$
	$g\left\{\hat{\chi}_{i,k}^+\right\} \le 0$
	$e\left\{\hat{\chi}_{\mathbf{i},\mathbf{k}}^+\right\} = 0$

Unscented Kalman Filter

The UKF, as well as the EKF, is a recursive estimation technique. The application of the UT has the advantage that the state estimates and their error covariance matrix can be calculated using the exact nonlinear process and measurement models. The steps of the UKF algorithm are described in Table A.3.[10,30,16]

The weights W_i^m and W_i^c are calculated as follows:

$$W_0^{(m)} = \frac{\lambda}{n+\lambda} \tag{A.5}$$

$$W_0^{(c)} = \frac{\lambda}{n+\lambda} + 1 - \alpha^2 + \beta \tag{A.6}$$

$$W_i^{(m)} = W_i^{(c)} = \frac{\lambda}{2(n+\lambda)}, \quad i = 1, \ldots, 2n \tag{A.7}$$

Reformulated Constrained Unscented Kalman Filter

A potential disadvantage of the UKF is that it does not allow imposing constraints on the state estimations. Constraints in the states commonly appear in chemical processes, e.g. concentrations greater or equal to zero. An estimator like EKF or UKF may give rise to negative concentration estimates even though this is physically impossible.

Different strategies to enforce estimates to lie between bounds in a given state estimation method have been proposed in the literature.[17,32,33] One of them is the RCUKF,[16] whose algorithm is shown in Table A.4.

Unscented Recursive Nonlinear Dynamic Data Reconciliation

In the RCUKF, state estimation updates with online measurements are enforced to satisfy bounds. However, the sigma points, and the propagated sigma points and their mean, could still lie outside the desired constraints. A method that overcomes this problem was developed by Vachhani et al.[17] They reformulated the selection of the sigma points and weights of the UKF so that the former and their mean do not violate the state constraints. In this technique, the URNDDR, the sigma points used in the propagation step are located asymmetrically around the current mean $\overline{\mathbf{x}}$. The direction along which these points are selected is the same as in the UKF, but the step size for all the sigma points $\chi_i = 1, .., 2n$ are chosen according to

$$\theta_{ik} = \min\left(\sqrt{n+\kappa}, \theta_{1k}, \theta_{2k}\right) \tag{A.8}$$

$$\theta_{1k} = \min_{j:\left(\sqrt{P_k}\right)_i > 0} \left[\infty, \left(x_{uj} - \hat{x}_{k|k,j}\right) \Big/ \left(\sqrt{\mathbf{P}_k}\right)_i\right] \tag{A.9}$$

$$\theta_{2k} = \min_{j:\left(\sqrt{P_k}\right)_i < 0} \left[\infty, \left(x_{lj} - \hat{x}_{k|k,j}\right) \Big/ \left(\sqrt{\mathbf{P}_k}\right)_i\right] \tag{A.10}$$

Therefore, the sigma points are computed as

$$\boldsymbol{\chi}_0 = \overline{\mathbf{x}} \tag{A.11}$$

$$\boldsymbol{\chi}_i = \overline{\mathbf{x}} + \theta_{ik}\left(\sqrt{\mathbf{P}_{\mathbf{x}}}\right)_i, \quad i = 1, \ldots, n \tag{A.12}$$

Table A.5. Algorithm of the URNDDR.

Step	Equation
initialization	$\hat{\mathbf{x}}_0 = E[\mathbf{x_0}], \quad \mathbf{P}_0 = E\left[(\mathbf{x}_0-\hat{\mathbf{x}}_0)(\mathbf{x}_0-\hat{\mathbf{x}}_0)^{\mathrm{T}}\right]$
computation of sigma points	$\chi_k = \left[\hat{\mathbf{x}}_k \hat{\mathbf{x}}_k k + \theta_i\left(\sqrt{\mathbf{P}_k}\right)_i \hat{\mathbf{x}}_k k - \theta_i\left(\sqrt{\mathbf{P}_k}\right)_i\right]$
state estimation propagation	$\chi_k^- = \mathbf{F}[\chi_k, \mathbf{u}_k], \quad \hat{\mathbf{x}}_k^- \sum_{i=0}^{2L} W_i^{\mathrm{m}} \chi_k^-$
error covariance propagation	$\mathbf{P}_k^- = \sum_{i=0}^{2L} W_i^{\mathrm{c}}\left[\chi_{i,k}^- - \hat{\mathbf{x}}_k^-\right]\left[\chi_{i,k}^- - \hat{\mathbf{x}}_k^-\right]^{\mathrm{T}}$
state estimation update at t_k with on-line measurements	$\hat{\mathbf{x}}_k^- = \sum_{i=0}^{2L} W_i^{\mathrm{m}} \chi_{i,k}^+$
error covariance update at t_k with online measurements	$\mathbf{P}_k^+ = \sum_{i=0}^{2L} W_i\left[\chi_{i,k}^+ - \hat{\mathbf{x}}_k^+\right]\left[\chi_{i,k}^+ - \hat{\mathbf{x}}_k^+\right]^{\mathrm{T}}$
where χ_k^+ is obtained by solving the optimization problem	$\min_{\hat{\chi}_{i,k}^+} \left(\mathbf{y}_k - h\left\{\hat{\chi}_{i,k}^+\right\}\right)^{\mathrm{T}} \mathbf{R}^{-1}\left(\mathbf{y}_k - h\left\{\hat{\chi}_{i,k}^+\right\}\right) + \left(\hat{\chi}_{i,k}^+ - \chi_{i,k}^-\right)^{\mathrm{T}} (\mathbf{P}_k^-)^{-1}\left(\hat{\chi}_{i,k}^+ - \chi_{i,k}^-\right)$
	$\mathbf{x}_{\mathrm{L}} \le \hat{\chi}_{i,k}^+ \le \mathbf{x}_{\mathrm{U}}$
	$g\left\{\hat{\chi}_{i,k}^+\right\} \le 0$
	$e\left\{\hat{\chi}_{\mathbf{i},\mathbf{k}}^+\right\} = 0$

$$\chi_i = \overline{\mathbf{x}} + \theta_{ik}\left(\sqrt{\mathbf{P_x}}\right)_{i-n}, \quad i = n+1, \ldots, 2n \tag{A.13}$$

This ensures that none of the sigma points violate the bounds $\mathbf{x}_{uj}$ and $\mathbf{x}_{lj}$.

The weights for computing the mean and covariance are calculated as shown in Equation (A.14)

$$W_i = a\theta_i + b \tag{A.14}$$

The calculus of parameter a and b were derivate and reported in Vachhani et al.[17]

Acknowledgements: the authors wish to thank CONICET, UNS, and ANPCyT for financial support.

Received: December 30, 2010; Revised: April 5, 2011; Published online: June 3, 2011; DOI: 10.1002/mren.201000060

Keywords: delayed measurements; polymerization; simulations; state estimation; unscented Kalman filter

[1] J. R. Richards, J. P. Congalidis, *Comput. Chem. Eng.* **2006**, *30*, 1447.
[2] S. Tatiraju, M. Soroush, B. A. Ogunnaike, *AIChE J.* **1999**, *45*, 769.
[3] S. Narasimhan, C. Jordache, *Data Reconciliation and Gross Error Detection: An Intelligent Use of Process Data*, Gulf Publishing Co, Houston, Texas, USA **2000**.
[4] J. A. Romagnoli, M. C. Sánchez, *Data Processing and Reconciliation for Chemical Process Operations*, Academic Press, New York **2000**.
[5] G. E. Fonseca, M. A. Dubé, A. Penlidis, *Macromol. React. Eng.* **2009**, *3*, 327.
[6] H. Schuler, Z. Suzhen, *Chem. Eng. Sci.* **1985**, *40*, 1891.
[7] K. Y. Choi, A. A. Khan, *Chem. Eng. Sci.* **1988**, *43*, 749.
[8] A. Sirohi, K. Y. Choi, *Ind. Eng. Chem. Res.* **1996**, *35*, 1332.
[9] R. K. Mutha, W. R. Cluett, A. Penlidis, *AIChE J.* **1997**, *43*, 3042.
[10] D. Li, M. C. Grady, R. A. Hutchinson, *Ind. Eng. Chem. Res.* **2005**, *44*, 2506.
[11] S. J. Julier, J. K. Uhlmann, *IEEE* **2004**, *92*, 401.
[12] J. Rawlings, B. B. Bakshi, R, *Comput. Chem. Eng.* **2006**, *30*, 1529.
[13] T. Chen, J. Morris, E. Martin, *J. Process Control* **2005**, *15*, 665.
[14] S. J. Julier, J. K. Uhlmann, *Proc. IEEE* **2004**, *92*, 401.
[15] N. Tudoroiu, K. Khorasani, in: *ICIECA 2005: International Conference on Industrial Electronics and Control Applications 2005*, Quito, Per **2005**.
[16] R. Galdeano, M. Asteasuain, M. Sánchez, in: *2009 AIChE Annual Meeting*, Nashville, TN **2009**.
[17] P. Vachhani, S. Narasimhan, R. Rengaswamy, *J. Process Control* **2006**, *16*, 1075.
[18] S. Kolås, B. Foss, A, T. Schei, S, *Comput. Chem. Eng.* **2009**, *33*, 1386.
[19] T. S. Schei, *J. Process Control* **2008**, *18*, 821.
[20] K. J. Kim, *PhD Thesis*, University of Maryland, **1991**.
[21] X. Lu, H. Zhang, W. Wang, K. Teo, L, *Automatica* **2005**, *41*, 1455.
[22] A. Hermoso-Carazo, J. Linares-Pérez, *Appl. Math. Model.* **2009**, *33*, 3705.
[23] C. Scali, M. Morretta, D. Semino, *J. Process Control* **1997**, *7*, 357.
[24] R. K. Mutha, W. R. Cluett, A. Penlidis, *Ind. Eng. Chem. Res.* **1997**, *36*, 1036.
[25] W. H. Ray, *Advanced Process Control*, McGraw-Hill, New York **1981**.
[26] N. Zambare, M. Soroush, M. C. Grady, *AIChE J.* **2002**, *48*, 1022.

[27] J. P. Congalidis, J. R. Richards, W. H. Ray, *AIChE J.* **1989**, *35*, 891.
[28] A. D. Schidt, W. H. Ray, *Chem. Eng. Sci.* **1981**, *36*, 1401.
[29] B. A. Ogunnaike, W. H. Ray, *Process Dynamics, Modeling, and Control*, Oxford University Press, Oxford, UK **1994**.
[30] D. Simon, *Optimal State Estimation: Kalman, H [infinity] and Nonlinear Approaches*, John Wiley & Sons, Inc., Hoboken, New Jersey, USA **2006**.
[31] S. J. Julier, J. K. Uhlmann, *AeroSense: The 11th International Symposium on Aerospace/Defense Sensing, Simulation and Controls*, Orlando, FL, USA **1997**.
[32] B. O. S. Teixeira, L. A. B. Tôrres, L. A. Aguirre, D. S. Bernstein, *J. Process Control* **2010**, *20*, 45.
[33] P. Vachhani, R. Rengaswamy, V. Gangwal, S. Narasimhan, *AIChE J.* **2005**, *51*, 946.